REPORT 03/2024

Application of acidic resins with new formulations as catalysts in solketal synthesis

Leandro Aguiar

Mathematical Modeling

1. Copolymerization model

Assumptions

- The sequences distributions are considered to be the same in soluble and gel polymer;
- The distribution of sequences containing only styrene units connecting the extreme groups (L_{An} to L_{En}) is considered to be the same as the distribution containing styrene and / or DVB units;
- Only mono-radicals were considered;
- Terminal model.

1.1 Balance of species

Table 1 - Copolymerization steps

Reaction	Chemical equation
Initiator decomposition	$I \xrightarrow{k_d} 2R_0^{\cdot}$
Styrene Initiation	$R_0^{\cdot} + M_1 \xrightarrow{k_{I_1}} R^{\cdot}$
Divinylbenzene initiation	$R_0^{\cdot} + M_2 \xrightarrow{k_{I_2}} R^{\cdot} + PDB$
PDB initiation	$R_0^{\cdot} + PDB \xrightarrow{k_{P_3}} R^{\cdot}$
Styrene propagation	$R^{\cdot} + M_1 \xrightarrow{k_{P_1}} R^{\cdot}$
Divinylbenzene propagation	$R^{\cdot} + M_2 \xrightarrow{k_{P_2}} R^{\cdot} + PDB$
PDB propagation	$R^{\cdot} + PDB \xrightarrow{k_{P_3}} R^{\cdot}$
Termination	$R^{\cdot} + R^{\cdot} \xrightarrow{k_t} P$
	$R_0^{\cdot} + R^{\cdot} \xrightarrow{k_t} P$
	$R_0^{\cdot} + R_0^{\cdot} \xrightarrow{k_t} P$

I: Initiator, $R_0^{\cdot}$: Primary radical, M_j: Monomer of type j, $R^{\cdot}$: Polymeric radical, PDB: Pendent double bond, P: Dead polymer, k_d to k_t: Rate constants of the reactions.

$$\frac{dI}{dt} = -k_d I \tag{1}$$

$$\frac{dR_0^{\cdot}}{dt} = 2fk_d I - k_{I_1} R_0^{\cdot} M_1 - k_{I_2} R_0^{\cdot} M_2 - k_{P_3} R_0^{\cdot} PDB - k_t R_0^{\cdot}(R_0^{\cdot} + R^{\cdot}) \tag{2}$$

$$\frac{dR^{\cdot}}{dt} = k_{I_1} R_0^{\cdot} M_1 + k_{I_2} R_0^{\cdot} M_2 + k_{P_3} R_0^{\cdot} PDB - k_t R^{\cdot 2} \tag{3}$$

$$\frac{dPDB}{dt} = k_{I_2} R_0^{\cdot} M_2 + k_{P_2} R^{\cdot} M_2 - k_{P_3} PDB(R_0^{\cdot} + R^{\cdot}) - \sum_{r=3}^{n_{max}} k_{cyc} L_{Ar} \tag{4}$$

$$\frac{dM_1}{dt} = -k_{I_1} R_0^{\cdot} M_1 - k_{P_1} R^{\cdot} M_1 \tag{5}$$

$$\frac{dM_2}{dt} = -k_{I_2} R_0^{\cdot} M_2 - k_{P_2} R^{\cdot} M_2 \tag{6}$$

In order to estimate the content of soluble chains occluded in the polymer network, balances for linear chain were carried out as follows.

$$\frac{dR_L^{\cdot}}{dt} = k_{I_1} R_0^{\cdot} M_1 - k_{P_2} R_L^{\cdot} M_2 - k_{P_3} R_L^{\cdot} PDB - k_t R_L^{\cdot 2} \tag{7}$$

$$\frac{dP_L}{dt} = \frac{k_t}{2} R_L^{\cdot 2} \tag{8}$$

$$\frac{dP}{dt} = \frac{k_t}{2} R^{\cdot 2} \tag{9}$$

The fraction of occluded soluble chains can be calculated through equation 10.

$$w_p = \frac{P_L}{P} \tag{10}$$

Where $R_L^{\cdot}$ is the concentration of linear radicals and P_L and P are the concentrations of linear and total polymer chains.

1.2 Balance of sequences

Table 2 - Reactions in terms of sequences

Chemical equations		
$R_0^{\cdot} + M_1 \xrightarrow{k_{I_1}} R_S^{\cdot}$	$L_{Ar} + L_{C_S} \xrightarrow{k_t} L_{D_{r+s}}$	$R_S^{\cdot} + L_{Ar} \xrightarrow{k_t} F$
$R_S^{\cdot} + M_1 \xrightarrow{k_{P_1}} R_S^{\cdot}$	$L_{Ar} + L_{A_S} \xrightarrow{k_{P_3}} L_{C_r} + L_{C_0} + L_{D_S}$	$R_S^{\cdot} + L_{C_r} \xrightarrow{k_t} F$
$R_0^{\cdot} + M_2 \xrightarrow{k_{I_2}} L_{A_0}$	$L_{Ar} + L_{B_S} \xrightarrow{k_{P_3}} L_{D_r} + L_{D_S} + L_{C_0}$	$R_S^{\cdot} + L_{Ar} \xrightarrow{k_{P_3}} L_{C_r} + L_{C_0}$

$$R_S^{\cdot} + M_2 \xrightarrow{k_{P_2}} L_{A_0} \qquad\qquad L_{A_r} + L_{D_s} \xrightarrow{k_{P_3}} L_{D_r} + L_{E_s} + L_{C_0} \qquad\qquad R_S^{\cdot} + L_{B_r} \xrightarrow{k_{P_3}} L_{D_r} + L_{C_0}$$

$$R_S^{\cdot} + R_S^{\cdot} \xrightarrow{k_t} P \qquad\qquad L_{C_r} + L_{A_s} \xrightarrow{k_{P_3}} L_{E_r} + L_{C_s} + L_{C_0} \qquad\qquad R_S^{\cdot} + L_{D_r} \xrightarrow{k_{P_3}} L_{E_r} + L_{C_0}$$

$$L_{A_r} + M_1 \xrightarrow{k_{P_1}} L_{A_{r+1}} \qquad\qquad L_{C_r} + L_{B_s} \xrightarrow{k_{P_3}} L_{E_r} + L_{D_s} + L_{C_0} \qquad\qquad R_0^{\cdot} + L_{A_r} \xrightarrow{k_{P_3}} L_{C_r} + L_{C_0}$$

$$L_{A_r} + M_2 \xrightarrow{k_{P_2}} L_{B_r} + L_{A_0} \qquad\qquad L_{C_r} + L_{D_s} \xrightarrow{k_{P_3}} L_{E_r} + L_{E_s} + L_{C_0} \qquad\qquad R_0^{\cdot} + L_{B_r} \xrightarrow{k_{P_3}} L_{D_r} + L_{C_0}$$

$$L_{C_r} + M_1 \xrightarrow{k_{P_1}} L_{C_{r+1}} \qquad\qquad L_{C_r} + L_{C_s} \xrightarrow{k_t} L_{E_{r+s}} \qquad\qquad R_0^{\cdot} + L_{D_r} \xrightarrow{k_{P_3}} L_{E_r} + L_{C_0}$$

$$L_{C_r} + M_2 \xrightarrow{k_{P_2}} L_{D_r} + L_{A_0} \qquad\qquad R_0^{\cdot} + L_{A_r} \xrightarrow{k_t} F \qquad\qquad L_{A_r} \xrightarrow{k_{cyc}} Cy_r + L_{C_0}$$

$$L_{A_r} + L_{A_s} \xrightarrow{k_t} L_{B_{r+s}} \qquad\qquad R_0^{\cdot} + L_{C_r} \xrightarrow{k_t} F$$

$R_0^{\cdot}$: Primary radical, M_1: Vinyl monomer (Styrene), M_2: Divinyl monomer (Divinylbenzene – DVB), $R_S^{\cdot}$: Polymeric radical containing only styrene units, P: Dead Polymer, F: Polymer fragment, L_{A_r} to L_{E_r}: Sequences containing r repeating units, Cy_r: cyclic chain containing r units.

$$\frac{dR_S^{\cdot}}{dt} = k_{I_1}R_0^{\cdot}M_1 - k_{P_2}R_S^{\cdot}M_2 - k_{P_3}R_S^{\cdot}\left(\sum_{r=0}^{n_{max}} L_{A_r} + 2\sum_{r=0}^{n_{max}} L_{B_r} + \sum_{r=0}^{n_{max}} L_{D_r}\right) -$$
$$k_t R_S^{\cdot}\left(\sum_{r=0}^{n_{max}} L_{A_r} + \sum_{r=0}^{n_{max}} L_{C_r}\right) - k_t R_S^{\cdot 2} \tag{11}$$

$$\frac{dL_{A_0}}{dt} = k_{I_2}R_0^{\cdot}M_2 + k_{P_2}M_2\left(\sum_{r=0}^{n_{max}} L_{A_r} + \sum_{r=0}^{n_{max}} L_{C_r} + R_S^{\cdot}\right) - L_{A_0}\Big[k_{P_1}M_1 + k_{P_2}M_2 +$$
$$k_t\left(\sum_{r=0}^{n_{max}} L_{A_r} + \sum_{r=0}^{n_{max}} L_{C_r} + R_0^{\cdot} + R_S^{\cdot}\right) + k_{P_3}\Big(2\sum_{r=0}^{n_{max}} L_{A_r} + 2\sum_{r=0}^{n_{max}} L_{B_r} + \sum_{r=0}^{n_{max}} L_{C_r} +$$
$$\sum_{r=0}^{n_{max}} L_{D_r} + R_0^{\cdot} + R_S^{\cdot}\Big)\Big] \tag{12}$$

$$\frac{dL_{A_r}}{dt} = k_{P_1}M_1 L_{A_{r-1}} - k_{P_1}M_1 L_{A_r} - k_{P_2}M_2 L_{A_r} - k_t L_{A_r}\left(\sum_{s=0}^{n_{max}} L_{A_s} + \sum_{s=0}^{n_{max}} L_{C_s} + R_S^{\cdot} + R_0^{\cdot}\right) -$$
$$k_{P_3}L_{A_r}\left(2\sum_{s=0}^{n_{max}} L_{A_s} + 2\sum_{s=0}^{n_{max}} L_{B_s} + \sum_{s=0}^{n_{max}} L_{C_s} + \sum_{s=0}^{n_{max}} L_{D_s} + R_S^{\cdot} + R_0^{\cdot}\right) - k_{cyc}L_{A_r}$$
$$\tag{13}$$

$$\frac{dL_{B_0}}{dt} = k_{P_2}L_{A_0}M_2 + \frac{1}{2}k_t L_{A_0}^2 - 2k_{P_3}L_{B_0}\left(\sum_{r=0}^{n_{max}} L_{A_r} + \sum_{r=0}^{n_{max}} L_{C_r} + R_0^{\cdot} + R_S^{\cdot}\right) \tag{14}$$

$$\frac{dL_{B_r}}{dt} = k_{P_2}L_{A_r}M_2 + \frac{1}{2}k_t\sum_{s=1}^{r} L_{A_s}L_{A_{r-s}} - 2k_{P_3}L_{B_r}\left(\sum_{s=0}^{n_{max}} L_{A_s} + \sum_{s=0}^{n_{max}} L_{C_s} + R_0^{\cdot} + R_S^{\cdot}\right) \tag{15}$$

$$\frac{dL_{C_0}}{dt} = -k_{P_1}L_{C_0}M_1 - k_{P_2}L_{C_0}M_2 - k_t L_{C_0}\left(\sum_{s=0}^{n_{max}} L_{A_s} + \sum_{s=0}^{n_{max}} L_{C_s} + R_S^{\cdot} + R_0^{\cdot}\right) -$$
$$k_{P_3}L_{C_0}\left(\sum_{s=0}^{n_{max}} L_{A_s} + 2\sum_{s=0}^{n_{max}} L_{B_s} + \sum_{s=0}^{n_{max}} L_{D_s}\right) + k_{P_3}\sum_{r=0}^{n_{max}} L_{A_r}\Big(2\sum_{r=0}^{n_{max}} L_{A_s} +$$
$$2\sum_{s=0}^{n_{max}} L_{B_s} + \sum_{s=0}^{n_{max}} L_{C_s} + \sum_{s=0}^{n_{max}} L_{D_s} + R_S^{\cdot} + R_0^{\cdot}\Big) + 2k_{P_3}\sum_{r=0}^{n_{max}} L_{B_r}\Big(\sum_{s=0}^{n_{max}} L_{C_s} + R_S^{\cdot} +$$
$$R_0^{\cdot}\Big) + k_{P_3}\sum_{r=0}^{n_{max}} L_{D_r}\left(\sum_{s=0}^{n_{max}} L_{C_s} + R_S^{\cdot} + R_0^{\cdot}\right) + k_{cyc}\sum_{r=3}^{n_{max}} L_{A_r} \tag{16}$$

$$\frac{dL_{C_r}}{dt} = k_{P_1}L_{C_{r-1}}M_1 - k_{P_1}L_{C_r}M_1 - k_{P_2}L_{C_r}M_2 - k_t L_{C_r}\left(\sum_{s=0}^{n_{max}} L_{A_s} + \sum_{s=0}^{n_{max}} L_{C_s} + R_S^{\cdot} + R_0^{\cdot}\right) - k_{P_3}L_{C_r}\left(\sum_{s=0}^{n_{max}} L_{A_s} + 2\sum_{s=0}^{n_{max}} L_{B_s} + \sum_{s=0}^{n_{max}} L_{D_s}\right) + k_{P_3}L_{A_r}\left(\sum_{s=0}^{n_{max}} L_{A_s} + \sum_{s=0}^{n_{max}} L_{C_s} + R_S^{\cdot} + R_0^{\cdot}\right) \tag{17}$$

$$\frac{dL_{D_0}}{dt} = k_{P_2}M_2 L_{C_0} + k_t L_{A_0}L_{C_0} + k_{P_3}L_{A_0}\left(2\sum_{s=0}^{n_{max}} L_{B_s} + \sum_{s=0}^{n_{max}} L_{D_s} + \sum_{s=0}^{n_{max}} L_{A_s}\right) + 2k_{P_3}L_{B_0}\left(\sum_{s=1}^{n_{max}} L_{A_s} + \sum_{s=0}^{n_{max}} L_{C_s} + R_0^{\cdot} + R_S^{\cdot}\right) - k_{P_3}L_{D_0}\left(\sum_{s=0}^{n_{max}} L_{A_s} + \sum_{s=0}^{n_{max}} L_{C_s} + R_0^{\cdot} + R_S^{\cdot}\right) \tag{18}$$

$$\frac{dL_{D_r}}{dt} = k_{P_2}L_{C_r}M_2 + k_t \sum_{s=1}^{r} L_{A_s}L_{C_{r-s}} + k_{P_3}L_{A_r}\left(2\sum_{s=0}^{n_{max}} L_{B_s} + \sum_{s=0}^{n_{max}} L_{D_s} + \sum_{s=0}^{n_{max}} L_{A_s}\right) + 2k_{P_3}L_{B_r}\left(\sum_{s=0}^{n_{max}} L_{A_s} + \sum_{s=0}^{n_{max}} L_{C_s} + R_S^{\cdot} + R_0^{\cdot}\right) - k_{P_3}L_{D_r}\left(\sum_{s=0}^{n_{max}} L_{A_s} + \sum_{s=0}^{n_{max}} L_{C_s} + R_S^{\cdot} + R_0^{\cdot}\right) \tag{19}$$

$$\frac{dL_{E_0}}{dt} = k_{P_3}\left(L_{C_0} + L_{D_0}\right)\sum_{s=0}^{n_{max}} L_{A_s} + k_{P_3}L_{C_0}\left(2\sum_{s=0}^{n_{max}} L_{B_s} + \sum_{s=0}^{n_{max}} L_{D_s}\right) + k_{P_3}L_{D_0}\left(\sum_{s=1}^{n_{max}} L_{C_s} + R_0^{\cdot} + R_S^{\cdot}\right) + \frac{1}{2}k_t L_{C_0}^2 \tag{20}$$

$$\frac{dL_{E_r}}{dt} = k_{P_3}\sum_{s=0}^{n_{max}} L_{A_s}\left(L_{C_r} + L_{D_r}\right) + k_{P_3}L_{C_r}\left(2\sum_{s=0}^{n_{max}} L_{B_s} + \sum_{s=0}^{n_{max}} L_{D_s}\right) + k_{P_3}L_{D_r}\left(\sum_{s=0}^{n_{max}} L_{C_s} + R_S^{\cdot} + R_0^{\cdot}\right) + \frac{1}{2}k_t \sum_{s=1}^{r} L_{C_s}L_{C_{r-s}} \tag{21}$$

Equations 1-9 and 11-21 were numerically integrated in Scilab through the algorithm ode. The concentration of crosslinked units, $[CL]$; total units, $[U]$; styrene units, $[U_1]$; and DVB units, $[U_2]$ are equated in (22), (23), (24) and (25) respectively.

$$[CL] = M_{2,0} - M_2 - PDB \tag{22}$$

$$[U] = [U_1] + [U_2] \tag{23}$$

$$[U_1] = M_{1,0} - M_1 \tag{24}$$

$$[U_2] = M_{2,0} - M_2 \tag{25}$$

The fraction of crosslinked units (Y_{CL}) and the molecular weight between crosslinks ($\overline{M_C}$) are defined in equations 26 and 27.

$$Y_{CL} = \frac{[CL]}{[U]} \tag{26}$$

$$\overline{M_C} = \frac{\overline{M_U}}{Y_{CL}} \tag{27}$$

1.3 Swelling behavior

It is understood that the swelling of resins depends on its interaction with the solvent, cross-link density, among other variables. Karam and Tien (1985)[1] describe a theoretical calculation for the swelling index (SI) of a resin containing occlusions, in a given solvent, based on a modification of the Flory-Rehner equation. The referred algorithm is shown in 28-31.

$$ln(1 - v_R) + v_R + \mu_R v_R^2 + \frac{\rho_R V_1 v_R^{\frac{1}{3}}}{\overline{M_C} K^{\frac{4}{3}}} - [ln(1 - v_0) + v_0 + \mu_P v_0^2] = 0 \tag{28}$$

$$ln(1 - v_R) + v_R + \mu_R v_R^2 + \frac{\rho_R V_1 v_R^{\frac{1}{3}}(1+2K^2)}{3\overline{M_C} K^{\frac{4}{3}}} + \frac{(K+1)^3 + 2K^3}{2[(K+1)^3 - K^3]}\{ln(1 - v_P) + v_P + \mu_P v_P^2 - [ln(1 -$$

$$v_0) + v_0 + \mu_P v_0^2]\} \tag{29}$$

$$K = \frac{v_R}{v_P} \tag{30}$$

$$SI = 1 + \frac{\left[\frac{\rho_S}{\rho_R} w_R \left(\frac{1}{v_R} - 1\right) + \frac{\rho_S}{\rho_P} w_P \left(\frac{1}{v_P} - 1\right)\right]}{w_R + w_P} \tag{31}$$

Where the interaction parameters can be calculated as follows.

$$\mu_R = 0.34 + V_1 \frac{(\delta_s - \delta_R)^2}{RT} \tag{32}$$

$$\mu_P = 0.34 + V_1 \frac{(\delta_P - \delta_s)^2}{RT} \tag{33}$$

The system was fed with the experimental value of $\overline{M_C}$ and w_p, provided by the copolymerization model and $v_0 = 0$ (dissolved polymer in the supernate was neglected). The system of non-linear equations 28-31 with four unknowns (v_R, v_P, K and SI) was solved through the function fsolve in scilab. The sulfonated polystyrene density (ρ_{PSS}) was calculated through the method of Sewell (1973).[2] In the present work these densities of the resin (ρ_R) and occluded polystyenre (ρ_P) were calculated as a function of the Ion Exchange Capacity (IEC) of the resin, as follows.

$$\rho_R = \rho_P = \frac{[IEC]}{[IEC]_{max}} \rho_{PSS} + \left(1 - \frac{[IEC]}{[IEC]_{max}}\right) \rho_{PS} \tag{34}$$

For styrene-divinylbenzene sulfonated resin, $[IEC]_{max} = 5.43\ mmol\ g^{-1}$. All terms are described in the symbology section.

The Swelling index can also be calculated for a sulfonated resin, by considering the solubility parameter of sulfonated polysterene[3] in equations 32 and 33. Then the swelling index (SI) can be used to estimate the particle porosity (ε_p) and particle radius (R_p) during the catalytic synthesis of solketal, as follows.

$$\varepsilon_p = \frac{\rho_R(SI-1)}{\rho_R(SI-1)+\rho_s} \tag{35}$$

$$R_p = R_{p,dry}\sqrt[3]{\frac{\rho_R}{\rho_{app}}} \tag{36}$$

Where ρ_{app}, ρ_R and ρ_s are the apparent density (mass of resin per volume of swollen particle), the resin density (skeletal density) and the solution density, respectively. $R_{p,dry}$ and R_p are the radii of dry and swollen particle, respectively.

2. Heterogeneous catalysis model

Hypotheses

- Homogeneous liquid phase
- Constant activity coefficients for the compounds along time and space
- Isothermal reaction

2.1 Balance equations

$$\varepsilon_p \frac{\partial C_{p,i}}{\partial t} = \frac{1}{r^2}\frac{\partial}{\partial r}\left(D_{eff,i}r^2\frac{\partial C_{p,i}}{\partial r}\right) + (1-\varepsilon_p)\nu_i\rho_R r_A \tag{37}$$

$$\frac{\partial C_{b,i}}{\partial t} = -\left(\frac{1-\varepsilon_b}{\varepsilon_b}\right)\frac{3}{r_p}D_{eff,i}\frac{\partial C_{p,i}}{\partial r}\bigg|_{r=r_p} \tag{38}$$

Boundary conditions

$$t = 0 \qquad\qquad C_{b,i} = C_{b,i0} \tag{39}$$

$$t = 0 \qquad\qquad C_{p,i} = C_{p,i0} \tag{40}$$

$$r = 0 \qquad\qquad \frac{\partial C_{p,i}}{\partial r} = 0 \tag{41}$$

$$r = r_p \qquad\qquad C_{b,i} = C_{p,i}\big|_{r=r_p} \tag{42}$$

Discretization with 4 points along the radius r were carried out to transform equation 36 into a system of ordinary differential equations (ODEs) using finite differences method. Adaptative refinement was implemented considering $\Delta r = 0.0266R_P$ for the two layers adjacent to the particle surface (inner and outer), the other points were equally spaced along the particle as shown in Figure 1.
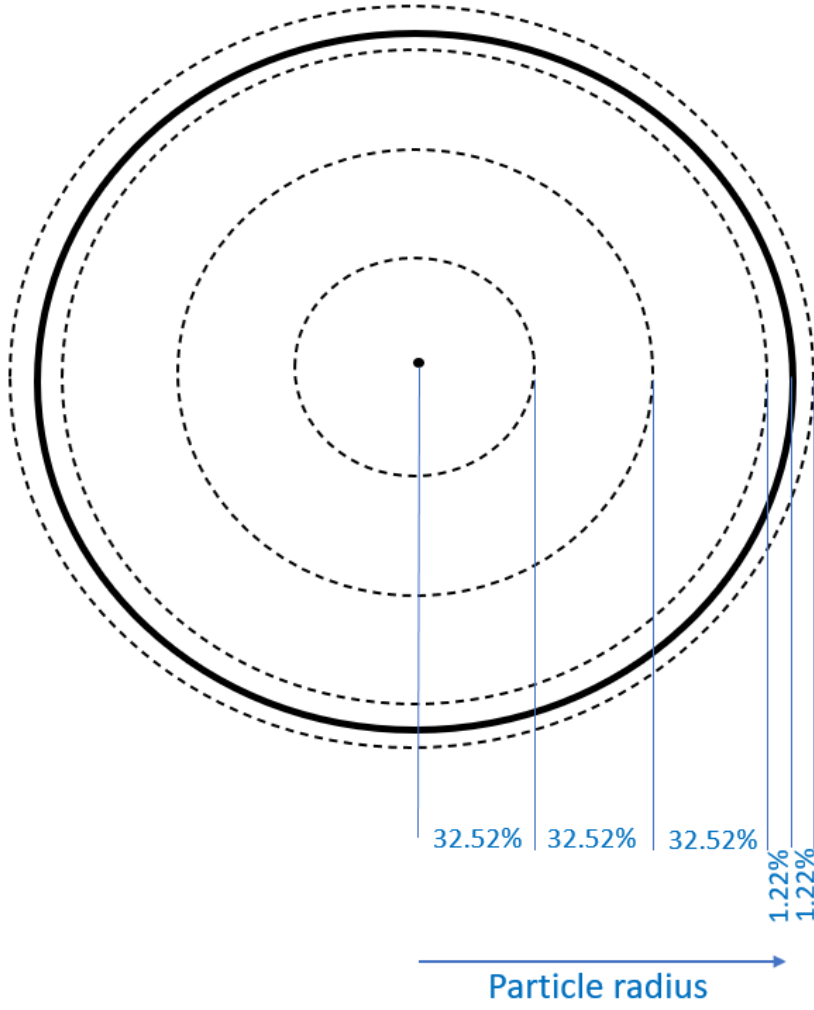
Figure 1 – Discretization with adaptative refinement.

The ODEs were numerically integrated along the reaction time through the algorithm ode in Scilab.

The effective diffusion coefficients were calculated through equation 43. Fernandez-Prini et al. (1976) described the tortuosity factor for a styrene-divinylbenzene sulfonated resin as $\tau = \frac{(2-\varepsilon_p)^2}{\varepsilon_p}$, which was used in the present study. [4]

$$D_{eff,i} = \frac{\varepsilon_p D_{i,m}}{\tau} \tag{43}$$

The diffusion coefficient of the component i in the mixture $(D_{i,m})$ was calculated through the Perkins and Geankoplis correlation[5] as follows.

$$D_{i,m} = \frac{1}{\eta_m^{0.8}} \sum_{\substack{j=1 \\ j \neq i}}^{nc} x_j D_{i,j}^0 \, \eta_j^{0.8} \tag{44}$$

The infinite dilution diffusivity of i in j is a function of temperature (T), viscosity of j (η_j) and the molar volumes of i and j ($V_{M,i}$ and $V_{M,j}$), and can be calculated for each pair of compounds in the mixture through equation 45.[6]

$$D_{i,j}^0 = \frac{8.2 \times 10^{-8} T}{\eta_j V_{M,i}^{\frac{1}{3}}} \left[1 + \left(\frac{3 V_{M,j}}{V_{M,i}} \right)^{\frac{2}{3}} \right] \tag{45}$$

The reaction rate of the limiting reagent consumption (r_A) was written considering the LHHW model in terms of activities as follows.

$$r_A = \frac{k_c \left(a_{Ac} a_{Gly} - \frac{a_{Solk} a_w}{K_{eq}} \right)}{\left(1 + K_{S,W} a_w \right)^2} \tag{46}$$

Applying the assumption of constant activity coefficient along the reaction, equation 47 can be written as:

$$r_A = \frac{k_c' \left(C_{Ac} C_{Gly} - \frac{C_{Solk} C_w}{K_{eq}'} \right)}{\left(1 + K_{S,W}' C_w \right)^2} \tag{47}$$

Where:

$$k_c' = k_c \frac{\gamma_{Ac} \gamma_{Gly}}{C_T^2} \tag{48}$$

$$K_{eq}' = \frac{\gamma_{Ac} \gamma_{Gly}}{\gamma_{Solk} \gamma_w} K_{eq} \tag{49}$$

$$K_{S,W}' = \frac{K_{S,W} \gamma_w}{C_T} \tag{50}$$

γ_i and C_i are the activity coefficient and concentration of the component i, respectively; C_T is the total concentration of compounds in the mixture. The activity coefficients used in equations 46 - 48 were calculated at the chemical equilibrium through UNIFAC, and the referred data are related in Appendix A.

The variation of k_c and K_{eq} with temperature were considered as follows.

$$k_c = k_{c0} exp\left[-\frac{E_a}{R} \left(\frac{1}{T} - \frac{1}{T_{ref}} \right) \right] \tag{51}$$

$$K_{eq} = \frac{\Delta S^o}{R} - \frac{\Delta H^o}{R} \frac{1}{T} \tag{52}$$

The reference temperature used in the present study was $T_{ref} = 313\,K$.

The parameter k_{c0} is the rate constant of the reaction catalyzed by a give resin at the reference temperature. This parameter can be correlated with the rate constant of the reaction at the catalytic site (k_{c0}^{s}) as described in equation (53).

$$k_{c0} = k_{c0}^{s}[CTI]_{eff} \tag{53}$$

Where $[CTI]_{eff}$ is the effective ion exchange capacity, i.e., the catalytic sites content that effectively participates in the reaction. Equation 54 shows its calculation.

$$[CTI]_{eff} = Y_{AS}[CTI] \tag{54}$$

Where Y_{AS} is the fraction of accessible sites in the resin. The accessibility to catalytic sites was assessed based on the molecular size of the compounds in the reaction medium and the radius of gyration of the sequences L_{E_r}. This radius of gyration of the sequences was estimated by considering the radius of a polystyrene chain in tetrahydrofuran at 25 °C, according to equation 55.[7]

$$R_g = 0.0118 M_w^{0.6} \tag{55}$$

In equation 55, M_w is the molecular weight of the chain in g mol^{-1} and R_g is the radius of gyration in nm. The comparison among molecular sizes is illustrated in Figure 2.
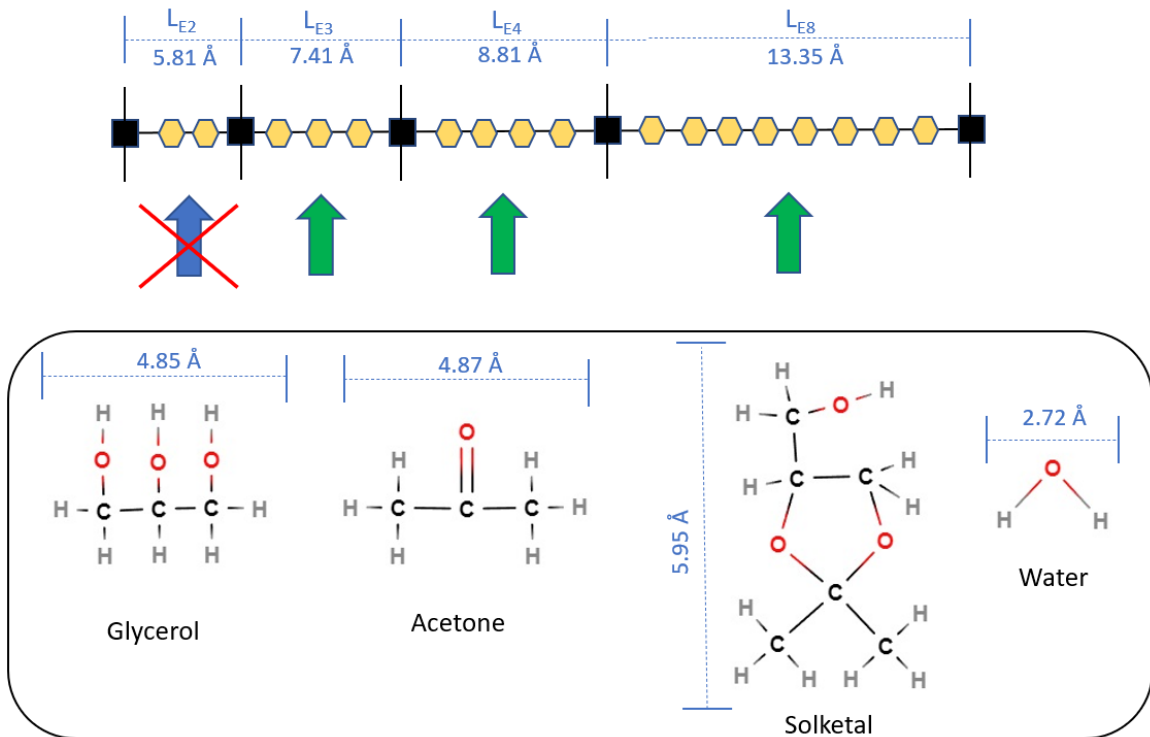

Figure 2 – Comparison among sequences and compounds molecular diameters.

In Figure 2, the molecular sizes of the compounds were estimated through Kim's expression, as described in equation 56.[8]

$$\sigma = 0.1363 V_M^{\frac{1}{3}} - 0.085 \tag{56}$$

Where σ is the molecular diameter in nm, and V_M is the molar volume in cm^3 mol^{-1}. This simplified analysis suggests that L$_{En}$ sequences with n ≤ 2 might be inaccessible due to hindering effects caused by the adjacent chains passing through the cross-linkages. The hindering effects can also be evaluated at free catalytic sites surrounded by occupied sites, as depicted in Figure 3.
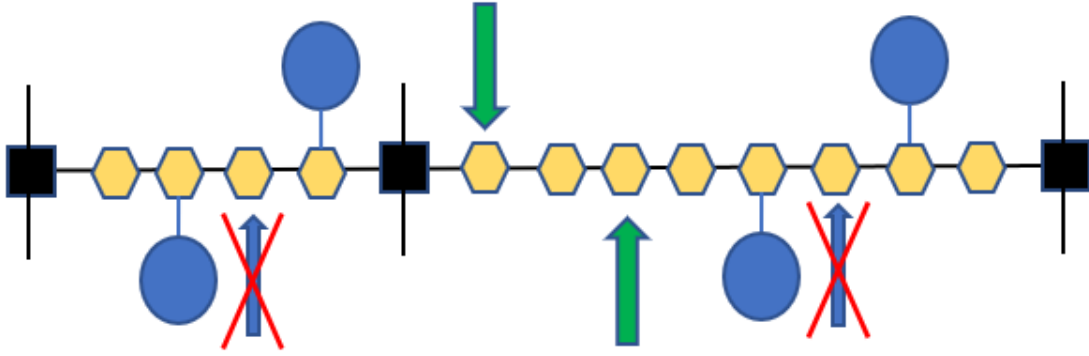

Figure 3 – Hindering effects caused by the occupied catalytic sites.

Considering that adjacent catalytic sites can not be occupied simultaneously (based on the molecular dimensions shown in Figure 2), the fraction of inaccessible sites can be estimated as follows.

$$Y_{AS} = (1 - Y_h) \frac{\sum_{n=3}^{n_{max}} L_{En}}{\sum_{n=1}^{n_{max}} L_{En}}$$

Where $\frac{\sum_{n=3}^{n_{max}} L_{En}}{\sum_{n=1}^{n_{max}} L_{En}}$ accounts for the sequences containing 3 or more units, and Y_h is the fraction of hindered units during the adsorption of molecules on the catalytic sites.

If $[CTI] \geq \frac{[CTI]_{max}}{2}$ then $Y_h = 1 - 0.5 \frac{[CTI]_{max}}{[CTI]}$

If $[CTI] < \frac{[CTI]_{max}}{2}$ then $Y_h = 0$

3. Results and discussion

3.1 Sensitivity analysis

Simulations were carried out considering the following data (unless otherwise stated):

Table 3 – Simulation data

Variable	Value
Number of discretization points (N)	4
Temperature	303 K
Molar ration acetone / glycerol	1
Ethanol percentage	50 % (mol)
Catalyst percentage	0.5 % (weight)
Particle diameter	412 μm

Thermodynamic data used in the model were collected from Moreira et al (2019).[9] $Y_{AS} = 0.57$; $\overline{M_C} = 1284\ g\ mol^{-1}$; $w_p = 0.0047$. Hindering effects due to the sites' occupation were neglected ($Y_h = 0$).

In order to conduct a sensitivity analysis for the model reaction variables and resin characteristics were studied as follows.

3.1 Effect of the resin characteristics

Firstly, simulations were carried considering constant and variable swelling indexes. The swelling index has a direct effect on the particle radius (R_P) and on its porosity (ε_P). The Figure 4 illustrates the results.
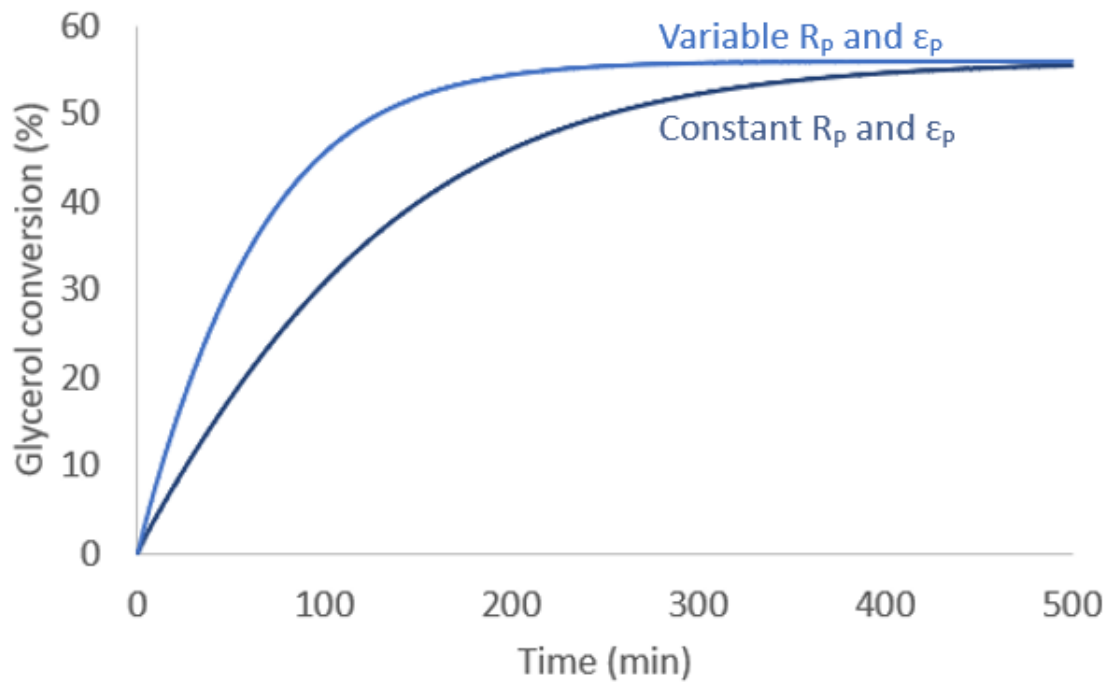

Figure 4 – Effect of the swelling index variation during the reaction.

The tortuosity in particulate systems can be a constant value or a function of the particle porosity. Figure 5 shows a comparison among the different approaches for tortuosity.
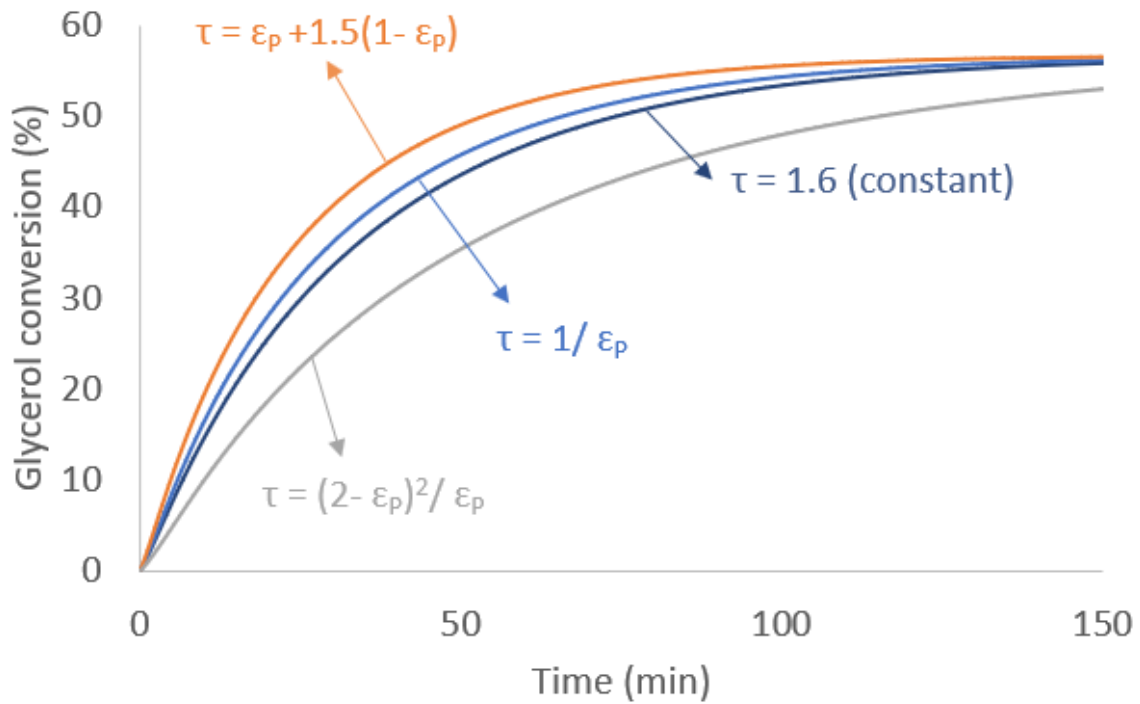

Figure 5 – Effect of Tortuosity.[4,10]

Figure 6 shows the effect of the particle size on the glycerol conversion.
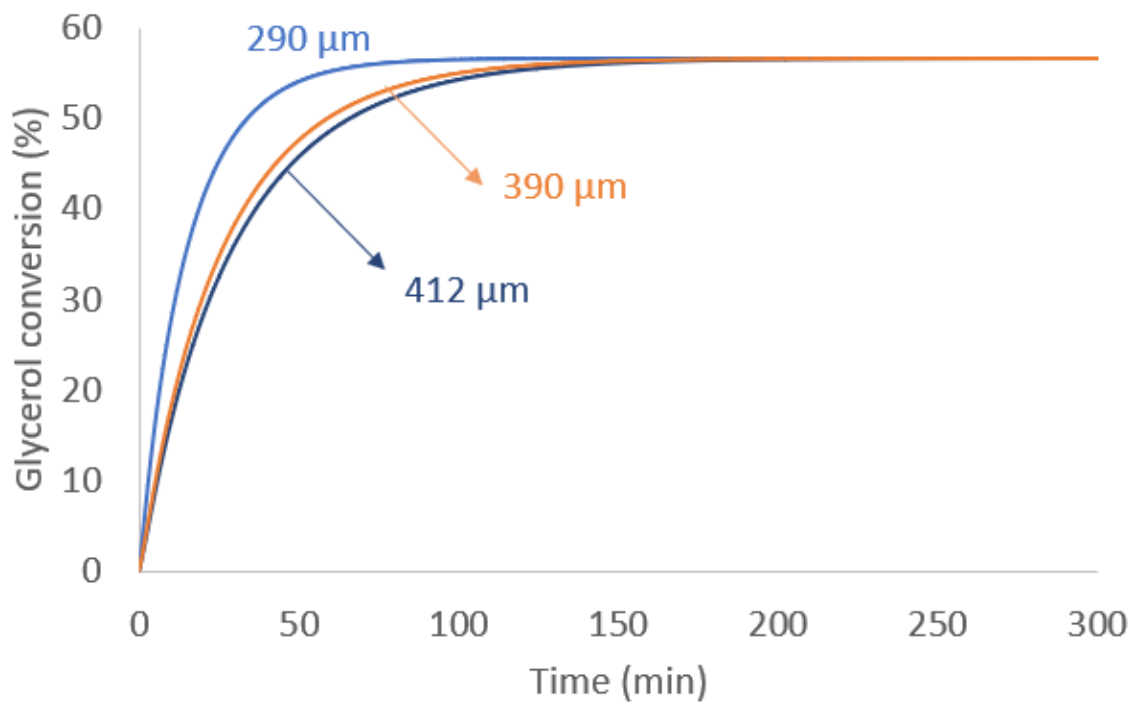

Figure 6 – Effect of particle size

3.2 Effect of reaction variables

The effects of temperature (T), acetone/glycerol molar ratio (MR) and catalyst content are illustrated in Figures 7, 8 and 9 respectively.
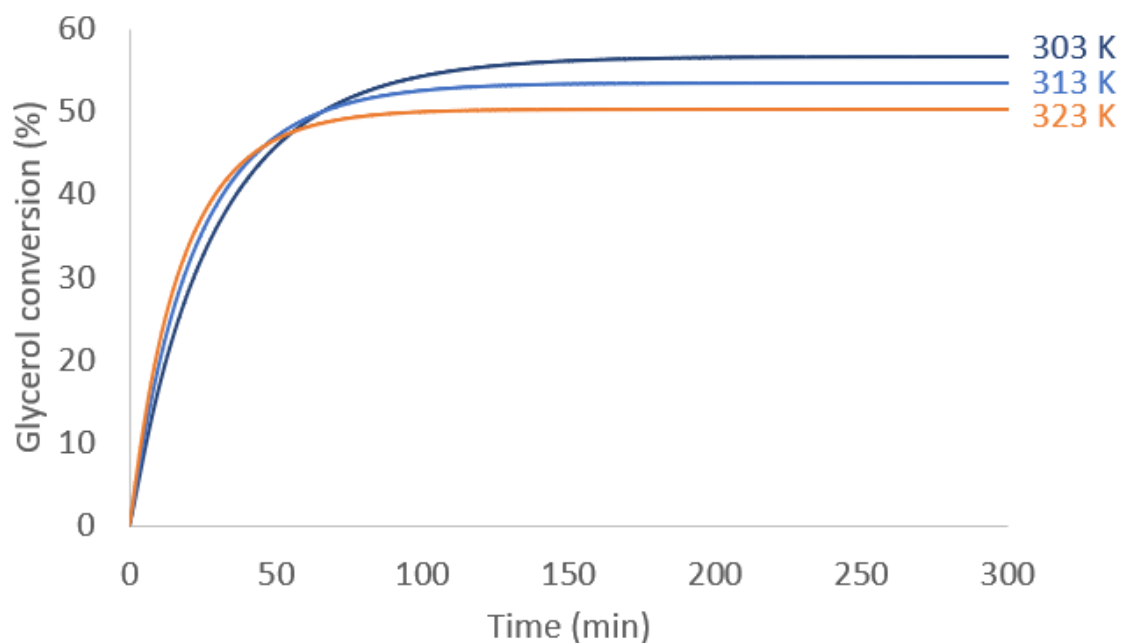

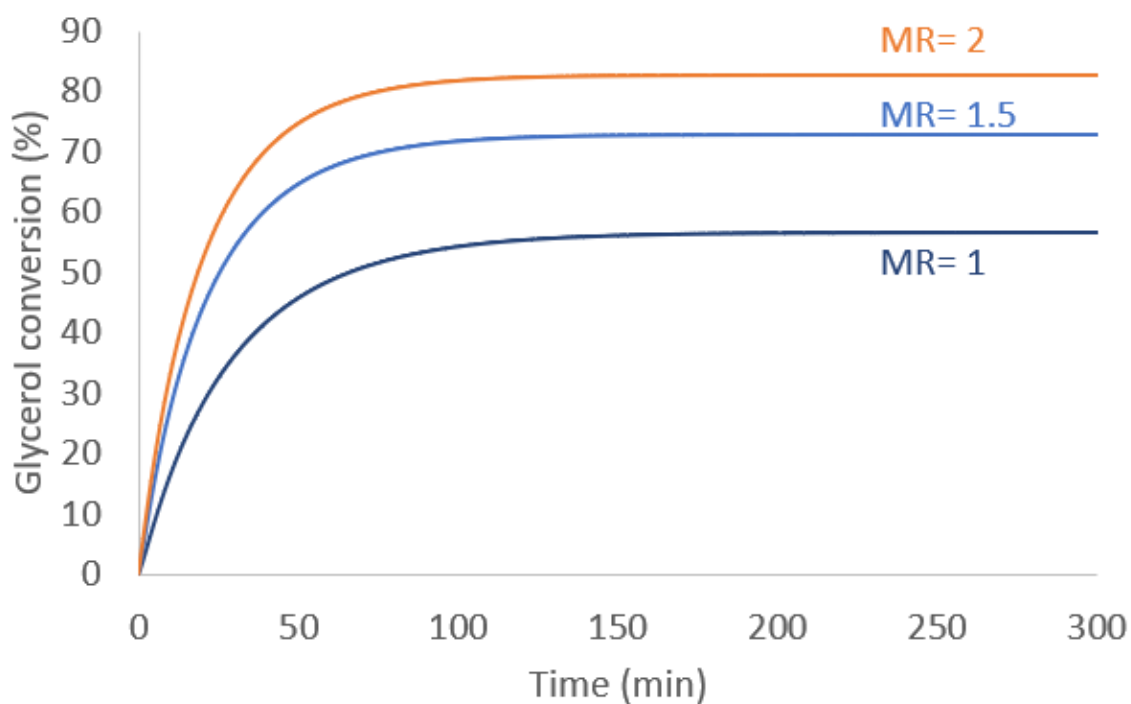Figure 7 – Effect of temperature

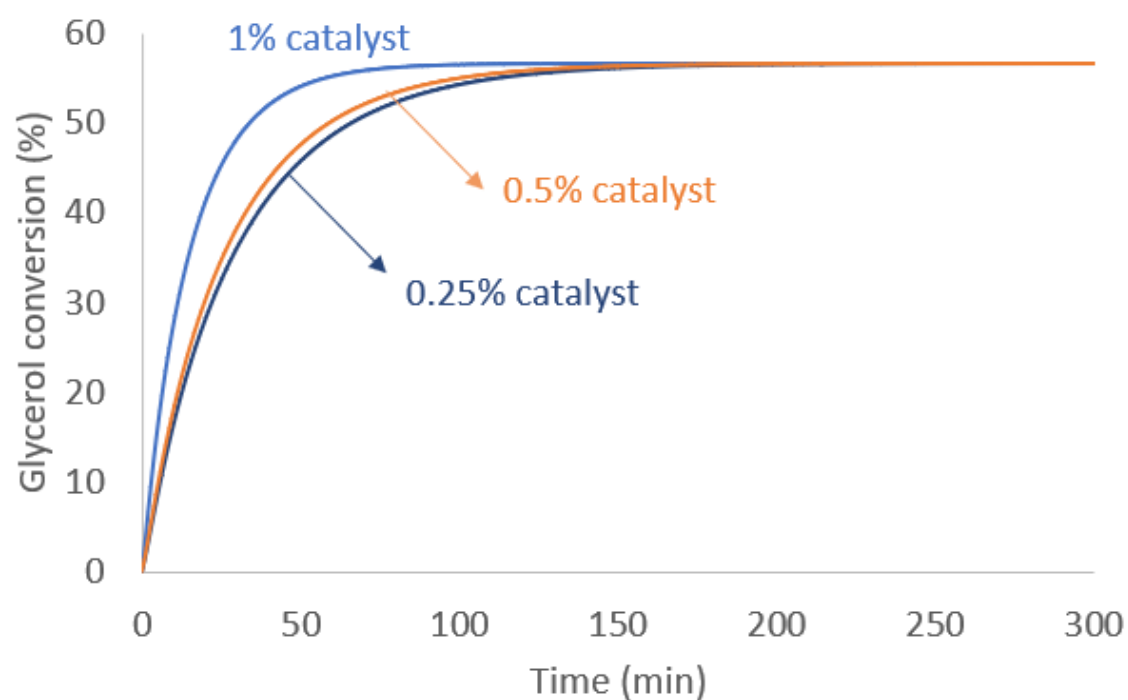
Figure 8 - Effect of acetone/glycerol molar ratio (MR).

Figure 9 – Effect of catalyst content

Figures 10 and 11 illustrate the effect of dilution and initial loading of the particles on the conversion results.
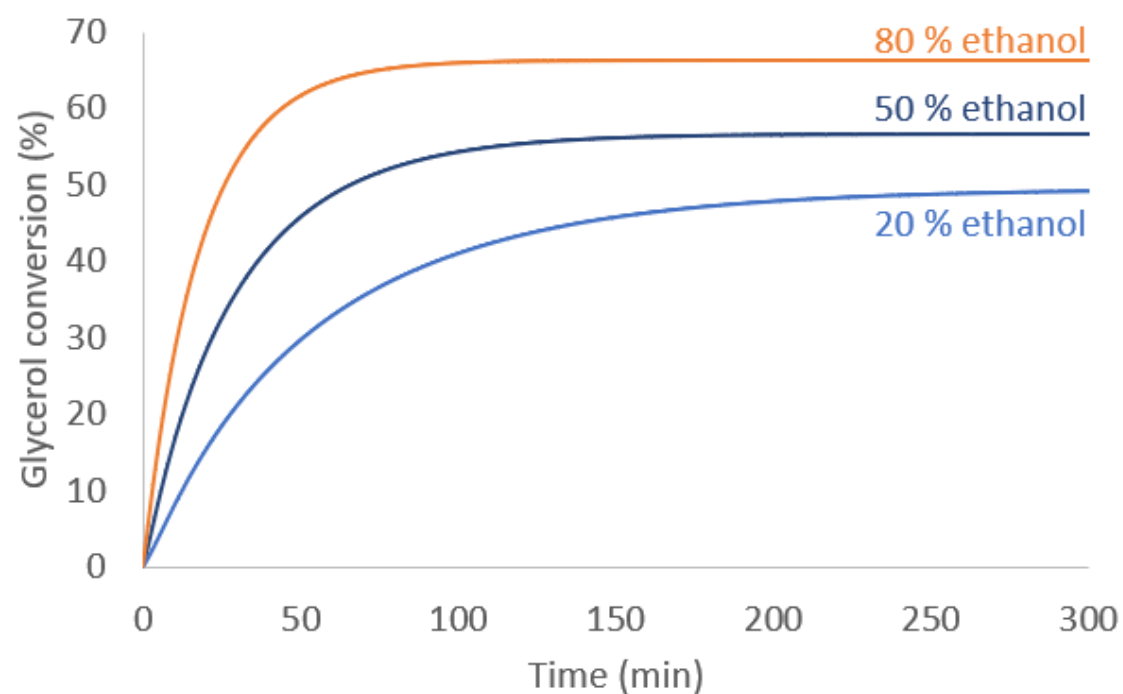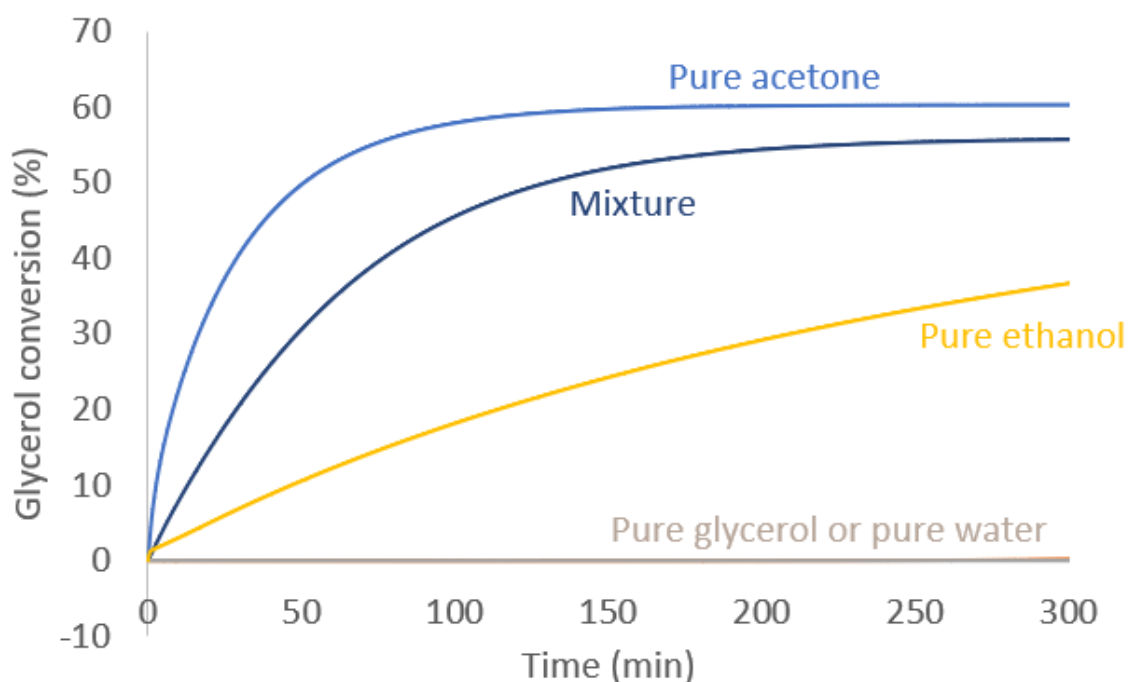

Figure 10 – Effect of dilution.

Figure 11 – Effect of initial particle loading

It is observed that considering particle swelling as described in section 2 has a considerable effect on the glycerol conversion curve compared to considering constant radius and porosity (as considered in literature studies) [11,12]. It is possible to notice that the tortuosity of sulfonated resin particles is higher compared to other tortuosity approaches, resulting in lower conversion over time. In Figure 11, the model prediction indicates that the initial loading of catalyst particles with acetone favors conversion. This behavior is associated with the acetone solubility parameter, which provides greater swelling, increasing the porosity of the particles. The model was also able to represent the decrease in reaction rate with increasing particle diameter, as expected for a diffusion-controlled process. Figures 7-9 present typical results of an exothermic reversible reaction (equilibrium conversion increases with decreasing temperature). Figure 10 indicates a strong effect of compound activity on conversion curves, prevailing over the effect of compound concentrations (see equations 47-50).

3.2 Model validation

The model was tested using experimental data from Moreira et al. (2019)[11], and the adjustments are illustrated in Figure 12.
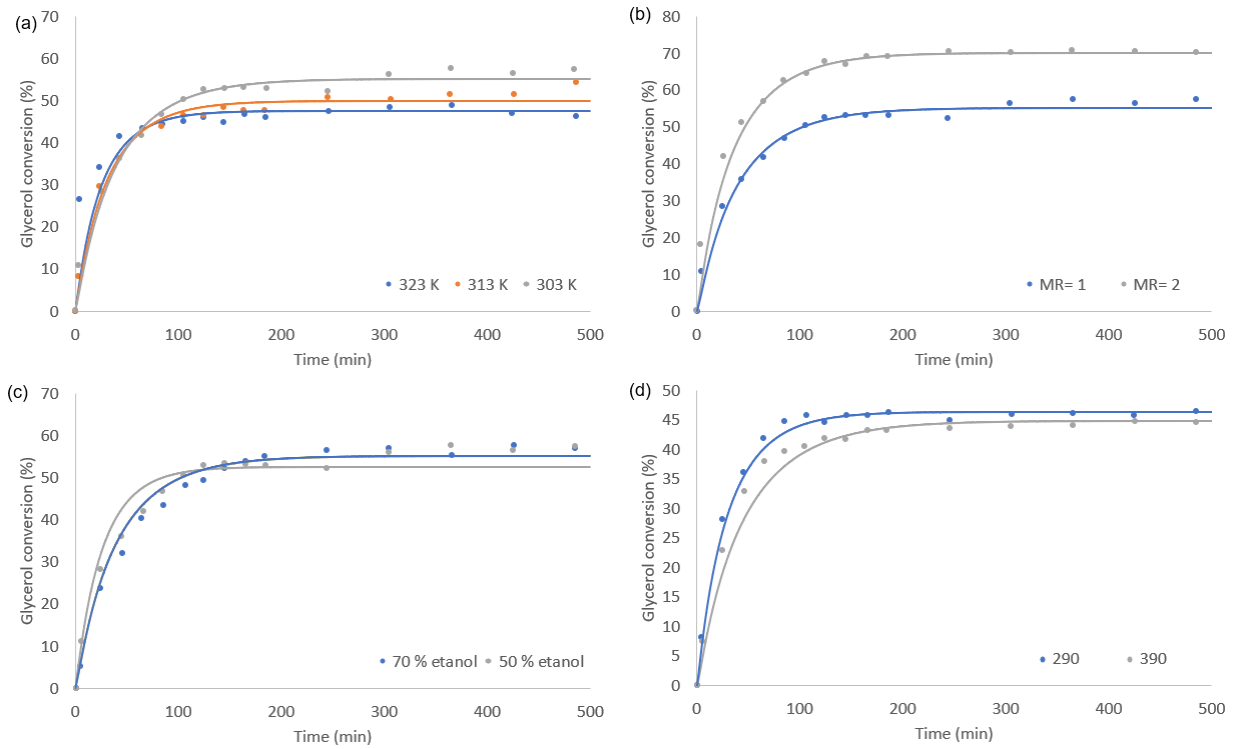
Figure 12 - Model fitting to experimental data from the literature.[11] (a) Temperature, (b) Acetone / glycerol molar ratio, (c) Ethanol percentage, (d) Particle diameter (μm).

It is observed in Figure 2.4 that the model generally represents the experimental profiles well. The optimal fit was obtained by minimizing the squared residuals, yielding an R^2 of 0.96. Table 4 presents the parameters used in this simulation and their differences from the literature values.

Table 4 - Parameters used in model validation.

Parameter	This study	Moreira et al. (2019)[11]
ΔH^o $(kJ\ mol^{-1})$	-25.53 ± 0.6	-20.10 ± 1.1
ΔG^o $(kJ\ mol^{-1})$	4.80 ± 0.9	1.40 ± 0.1
R^2	0.96	0.96

Os parâmetros cinéticos utilizados são os mesmos do modelo LHHW de Moreira et al. (2019)[11] $Y_{AS} = 0.57$; $\overline{M_C} = 1284\ g\ mol^{-1}$; $w_p = 0.0047$. Hindering effects due to the sites' occupation were neglected ($Y_h = 0$).

The discrepancies observed in Table 4 may be primarily associated with the differences between the methods used in the models. The present work used finite differences and modified UNIFAC, while the work of Moreira et al. (2019) used orthogonal collocation and the original UNIFAC

method. It is worth noting that the present model also takes into account particle swelling during the process.

4. Conclusion

Copolymerization modeling was carried out for the synthesis of the catalyst support through species and sequence balances, considering cyclization reactions and distinguishing between linear and crosslinked chains. Information provided by this model, such as the average molecular weight between cross-links and the fraction of soluble chains, were used to predict the swelling variation of the resin during its application. It is concluded from the simulations that considering the variation in particle size and porosity due to catalyst swelling produces the expected effect on simulated glycerol conversions. The adjustments with experimental data revealed an R^2 of 0.96, and the thermodynamic parameters found were close to literature values. Furthermore, the copolymerization model provides an indication of chain density through sequence size distributions, which will allow, in future studies, the evaluation of accessibility to catalytic sites as a function of resin synthesis conditions.

Symbology

Symbol	Description	Unit
C_i	Concentration of the component i	mol L^{-1}
C_{i0}	Initial concentration of the component i	mol L^{-1}
C_P	Reactivity correlation parameter	Dimensionless
$[CL]$	Crosslinked units concentration	mol L^{-1}
f	Initiator efficiency	Dimensionless
I	Initiator concentration	mol L^{-1}
IEC	Ion exchange capacity	meq g^{-1}
IEC_{eff}	Effective ion exchange capacity	meq g^{-1}
k_c	Rate constant of reaction	mol kg^{-1} s^{-1}
k_c'	Apparent rate constant of reaction	L^2 mol^{-1} kg^{-1} s^{-1}
k_{c0}	Rate constant for the reference temperature	mol kg^{-1} s^{-1}
K	Ratio $\frac{v_R}{v_P}$	Dimensionless
k_d	Initiator decomposition constant	s^{-1}

K_{eq}	Equilibrium constant of the reaction	Dimensionless
K'_{eq}	Apparent equilibrium constant	Dimensionless
k_{I_1}	Styrene initiation constant	L mol^{-1} s^{-1}
k_{I_2}	DVB initiation constant	L mol^{-1} s^{-1}
k_{p_1}	Styrene propagation constant	L mol^{-1} s^{-1}
k_{p_2}	DVB propagation constant	L mol^{-1} s^{-1}
k_{P_3}	PDB propagation constant	L mol^{-1} s^{-1}
$K_{S,W}$	Adsorption equilibrium constant for water	Dimensionless
$K'_{S,w}$	Apparent adsorption equilibrium constant	L mol^{-1}
k_t	Termination constant	L mol^{-1} s^{-1}
L_{A_r}	Concentrations of sequences containing r styrene units connecting a PDB to a radical center	mol L^{-1}
L_{B_r}	Concentration of sequences containing r styrene units connecting two PDBs	mol L^{-1}
L_{C_r}	Concentration of sequences containing r styrene units connecting a crosslinked unit to a radical center	mol L^{-1}
L_{D_r}	Concentration of sequences containing r styrene units connecting a PDB to a crosslinked unit	mol L^{-1}
L_{E_r}	Concentration of sequences containing r styrene units connecting two crosslinked units	mol L^{-1}
M_1	Styrene concentration	mol L^{-1}
$M_{1,0}$	Initial styrene concentration	mol L^{-1}
M_2	DVB concentration	mol L^{-1}
$M_{2,0}$	Initial DVB concentration	mol L^{-1}
$\overline{M_C}$	Average molecular weight between CLs	g mol^{-1}
$\overline{M_U}$	Average molecular weight of polymerized units	g mol^{-1}
n	Number of units between CLs	r.u.
n_{max}	Maximum n considered in the copolymerization modeling	r.u.
PDB	Pendant double bonds concentration	mol L^{-1}
$R^{\cdot}$	Total radicals' concentration	mol L^{-1}
$R_0^{\cdot}$	Primary radicals' concentration	mol L^{-1}
r_A	Rate of reaction for the limiting reagent	mol L^{-1} min^{-1}
R_P	Radius of swollen particle	dm
$R_{P,dry}$	Radius of dry particle	dm

$R_S^{\cdot}$	Concentration of radicals containing only styrene units	mol L^{-1}
SI	Swelling Index	Dimensionless
$[SU]$	Concentration of sulfonated units	mol L^{-1}
$[U]$	Concentration of total polymerized units	mol L^{-1}
$[U_1]$	Concentration of Styrene units	mol L^{-1}
$[U_2]$	Concentration of DVB units	mol L^{-1}
v_0	Volume fraction of dissolved polymer in the supernate	Dimensionless
V_1	Molar volume of solvent	cm³ mol^{-1}
v_P	Volume fraction of polystyrene in the swollen occluded polystyrene	Dimensionless
v_R	Volume fraction of rubber in the swollen rubber network	Dimensionless
w_P	Weight fraction of occluded polystyrene in the gel	Dimensionless
w_R	Weight fraction of rubber in the gel	Dimensionless
X_G	Glycerol conversion	Dimensionless
Y_{CL}	Fraction of crosslinked units	mol CL (mol U)$^{-1}$
$Y_{LE,n}$	Fraction of L_{E_n} among all L_E	mol L_{E_n} (mol total L_E)$^{-1}$
μ_R	Rubber-solvent interaction factor	Dimensionless
μ_P	Polystyrene-solvent interaction factor	Dimensionless
ρ_i	Density of i	kg dm^{-3}

References

1. Karam, H. J. & Tien, L. Analysis of swelling of crosslinked rubber gel with occlusions. *J Appl Polym Sci* **30**, 1969–1988 (1985).

2. Sewell, J. H. *A Method of Calculating Densities of Polymers*. *JOURNAL OF APPLIED POLYMER SCIENCE* vol. 17 (1973).

3. Ferrell, W. H., Kushner, D. I. & Hickner, M. A. Investigation of polymer–solvent interactions in poly(styrene sulfonate) thin films. *J Polym Sci B Polym Phys* **55**, 1365–1372 (2017).

4.   Fernandez-Prlni, R. & Philipp, M. *Diffusion Coefficients in Poly(Styrenesu1fonate) Resins Tracer Diffusion Coefficients of Counterions in Homo-and Heteroionic Poly(Styrenesu1fonate) Resins*.

5.   Perkins, L. R. & Geankoplis, C. J. *Molecular Diffusion in a Ternary Liquid System with the Diffusing Component Dilute. Chemical Engineering Science, 1%9* vol. 24.

6.   Andreas, J AI, Hauser & Tucker. *Fundamental Research on Occurrence and Recovery of Petroleum. Polytechnic Inst. Brooklyn, Tech. Rcpt* vol. 44 (1952).

7.   Terao, K. & Mays, J. W. On-line measurement of molecular weight and radius of gyration of polystyrene in a good solvent and in a theta solvent measured with a two-angle light scattering detector. *Eur Polym J* **40**, 1623–1627 (2004).

8.   Marcus, Y. The sizes of molecules - Revisited. *Journal of Physical Organic Chemistry* vol. 16 398–408 Preprint at https://doi.org/10.1002/poc.651 (2003).

9.   Moreira, M. N., Faria, R. P. V., Ribeiro, A. M. & Rodrigues, A. E. Solketal Production from Glycerol Ketalization with Acetone: Catalyst Selection and Thermodynamic and Kinetic Reaction Study. *Ind Eng Chem Res* **58**, 17746–17759 (2019).

10.   Barbosa, N. A. *et al. Simulated Moving Bed Separators/Reactors: Application to the Synthesis of 1,1-Dibutoxyethane (DBE)*. (2012).

11.   Moreira, M. N., Faria, R. P. V., Ribeiro, A. M. & Rodrigues, A. E. Solketal Production from Glycerol Ketalization with Acetone: Catalyst Selection and Thermodynamic and Kinetic Reaction Study. *Ind Eng Chem Res* **58**, 17746–17759 (2019).

12.   Esteban, J., Garciá-Ochoa, F. & Ladero, M. Solventless synthesis of solketal with commercially available sulfonic acid based ion exchange resins and their catalytic performance. *Green Processing and Synthesis* **6**, 79–89 (2017).

13.   Jakob, A., Grensemann, H., Lohmann, J. & Gmehling, J. Further development of modified UNIFAC (Dortmund): Revision and extension 5. *Ind Eng Chem Res* **45**, 7924–7933 (2006).

14.   DDBST GmbH. Parameters of the Modified UNIFAC (Dortmund) Model. *https://www.ddbst.com/PublishedParametersUNIFACDO.html. Accessed in January, 10* (2024).

APPENDIX A

The activity coefficients of the compounds in the reaction mixture were calculated through the modified UNIFAC model.[13] The groups used in the calculation are depicted in Figure A1.
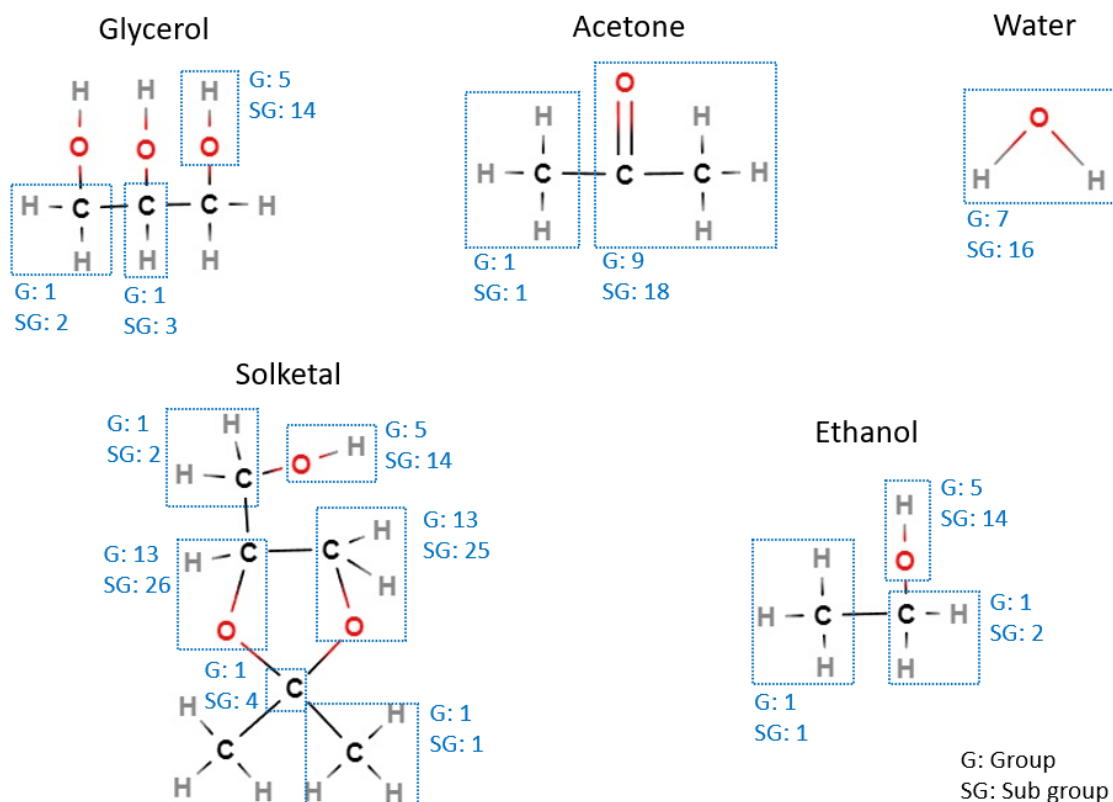
Figure A1 – Groups used in the calculation of activity coefficients.

The UNIFAC parameters were collected from Dortmund Data Bank[14] and are related in Tables A1-A4.

Table A1 – UNIFAC Structural groups

Group	Sub Group	Symbol	R	Q
1	1	CH3	0.6325	1.0608
1	2	CH2	0.6325	0.7081
1	3	CH	0.6325	0.3554
1	4	C	0.6325	0.0000
5	15	OH	1.2302	0.8927
9	18	CH3CO	1.7048	1.6700
13	25	CH2O	1.1434	1.2495
13	26	CHO	1.1434	0.8968
7	16	H2O	1.7334	2.4561

Table A2 – UNIFAC energy interaction parameter $a_{n,m}$

Group	1	5	9	13	7
1	0	2777	433.6	233.1	1391.3
5	1606	0	-250	816.7	-801.9
9	199	653.3	0	3645	770.6
13	-9.654	650.9	695.8	0	433.207
7	-17.253	1460	190.5	177.665	0

Table A3 – UNIFAC energy interaction parameter $b_{n,m}$

Group	1	5	9	13	7
1	0	-4.674	0.1473	-0.3155	-3.6156
5	-4.746	0	2.857	-5.092	3.824
9	-0.8709	-1.412	0	-26.91	-0.5873
13	-0.03242	-0.7132	-0.9619	0	-0.6053
7	0.8389	-8.673	-3.669	-3.7291	0

Table A4 – UNIFAC energy interaction parameter $c_{n,m}$

Group	1	5	9	13	7
1	0	1.55×10^{-3}	0	0	1.144×10^{-3}
5	9.181×10^{-4}	0	6.022×10^{-3}	6.065×10^{-3}	-7.514×10^{-3}
9	0	9.54×10^{-4}	0	0	-3.252×10^{-3}
13	0	8.15×10^{-4}	-2.462×10^{-3}	0	-9.14×10^{-4}
7	9.021×10^{-4}	0.01641	8.838×10^{-3}	0.010763	0

Table A5 – Activity coefficients along the reaction.

X_G	γ_{Gly}	γ_{Ac}	γ_{Solk}	γ_W	γ_E
0.1	2.93	4.55	0.77	0.73	1.19
0.2	2.95	4.37	0.85	0.95	1.18
0.3	2.95	4.14	0.92	1.18	1.16
0.4	2.94	3.90	0.99	1.42	1.13
0.5	2.92	3.64	1.04	1.65	1.10
0.6	2.88	3.38	1.08	1.88	1.07
0.7	2.84	3.13	1.12	2.10	1.04
0.8	2.80	2.89	1.15	2.30	1.01

X_G: glycerol conversion, γ_i: Activity coefficient of i.